Color of smoke from brush fires

David K. Lynch[1,*] and Lawrence S. Bernstein[2]

[1]Thule Scientific, 22914 Portage Circle Drive, Topanga, California 90290, USA

[2]Spectral Sciences, Incorporated, 4 Fourth Avenue, Burlington, Massachusetts 01803-3304

*Corresponding author: thule@earthlink.net

Received 17 March 2008; revised 3 July 2008; accepted 24 July 2008;
posted 24 July 2008 (Doc. ID 93821); published 23 September 2008

Smoke clouds from brush fires usually appear reddish or brownish when viewed from below in transmission, while a thin smoke cloud or part of a thick cloud near its periphery is noticeably bluish. Yet, when viewed from above in backscatter, the smoke appears bluish-white. We present observations of smoke clouds and explain their varied colors using a simple one-dimensional two-stream multiple scattering/absorbing radiative transfer approach for a model cloud whose particles are much smaller than the wavelength of visible light, the Rayleigh limit. The colors are purely the result of Rayleigh scattering and are not significantly influenced by the intrinsic color (wavelength-dependent albedo) of the particles.

OCIS codes: 010.1100, 010.1310, 010.1615, 010.1690, 010.7295, 010.5620.

1. Introduction

Forests and brush fires occur naturally throughout the world as a result of lightning strikes. Human activity such as crop burning and arson also produces forest fires. Observationally, smoke clouds in transmission appear reddish-brown, while in reflection they appear bluish or white (gray). Baleful red sunsets and brownish-tinged clouds are hallmarks of nearby fires. Individually, the particles of ash are nearly colorless (gray) and have a high single-scattering albedo, i.e., they appear white or very light gray. However, a collection of interacting particles, as occurs in a smoke cloud, can exhibit a wide range of colors. The observed color depends on the wavelength-dependent optical opacity of the cloud. We present observations of smoke clouds and show that their colors and brightness can be explained using a simple one-dimensional (1-D), two-stream, multiple scattering radiative transfer model.

2. Observations

Figure 1 shows a photograph of smoke from the brush fire in July of 2006 on the eastern flanks of the Cascade Mountains. The main part of the cloud is reddish-brown, while its thin outer extensions are bluish-white. In this picture the Sun is about 60° above the horizon and the gross Sun–cloud–observer scattering angle ranges from 0 to about 20°. Thus we are seeing transmitted light, i.e., downwelling radiation. Figure 2 shows a NASA image of Santa Ana wind-driven smoke in Southern California that has been blown over the ocean. It is obviously white or gray and certainly not reddish-brown. The color is representative of backscattered or upwelling radiation from the cloud. The authors have seen smoke from many such fires, and the fundamental properties are the same. Indeed, by entering "brush fire" into any search engine, hundreds of pictures will be returned that confirm our observations.

3. Radiative Transfer Model

For simplicity, we consider a very common smoke cloud geometry in which a cloud's vertical extent is much less than its horizontal extent, i.e., a pancake cloud. In this limit, the reflected and transmitted fluxes are well described by 1-D, two-stream radiative transfer models. In this study, we employ a 1-D multiple scattering model with a compact and exact analytical solution [1] that can be written explicitly for the upwelling $I/I_o\Uparrow(\lambda)$ and downwelling radiation

0003-6935/08/34H143-06$15.00/0

Fig. 1. In transmission, brush fire smoke appears reddish-brown except around the cloud's periphery where the optical depth is small. Here the smoke appears bluish or whitish. Photograph by Alan Beeler.

$I/I_o\Downarrow(\lambda)$ as

$$I/I_o\Downarrow(\lambda) = [e^{k(\tau_o-\tau)} - r_o^2 e^{-k(\tau_o-\tau)}]/e^{k\tau_o} - r_o^2 e^{-k\tau_o}] - e^{-\tau}, \quad (1)$$

$$I/I_o\Uparrow(\lambda) = r_o[e^{k(\tau_o-\tau)} - e^{-k(\tau_o-\tau)}]/e^{k\tau_o} - r_o^2 e^{-k\tau_o}], \quad (2)$$

where I is the scattered light, I_o is the incident light (sunlight), and λ is wavelength. τ is the optical depth at any point inside the cloud whose total optical depth is τ_o at a reference wavelength λ_o, here chosen as $0.5\,\mu$m. We have taken I_o to be a 5700 K Planck function to represent the incident solar sunlight. The extinction parameter k is

$$k = [(1-\omega_o)(1-g\omega_o)]^{1/2}, \quad (3)$$

where ω_o is the single-scattering albedo and g is the asymmetry parameter ($g = 0$ for isotropic and Rayleigh scattering and $+1$, -1 for perfect forward, backward scattering). The reflectivity term r_o is

$$r_o = (k-1+\omega_o)/(k+1-\omega_o). \quad (4)$$

Fig. 2. In reflection (backscatter) the smoke is whitish or bluish but not reddish-brown. Photograph courtesy of NASA, showing smoke from southern California brush fires.

Rayleigh scattering's wavelength dependence ($1/\lambda^4$) comes into the solution to Eqs. (1) and (2) through the optical depth. The vertical optical depth of the cloud $\tau_C(\lambda)$ is

$$\tau_C(\lambda) = \tau_o(\lambda_o/\lambda)^4. \quad (5)$$

At shorter wavelengths, the optical depth is significantly higher than it is at longer wavelengths. For example, when $\tau_o = 1$ at $\lambda_o = 0.5\,\mu$m, the cloud optical depths τ_C at 0.4 and $0.7\,\mu$m are 2.44 and 0.26, respectively. The justification for approximating the wavelength dependence of the extinction cross section of smoke particles as Rayleigh scatterers is based on their many measured and inferred size distributions, mainly from the SCAR-B experiment [2], which are representative. Mean geometric particle radii are in the range of 0.01–$0.05\,\mu$m [3–6], largely satisfying the Rayleigh limit that the wavelength of light is much larger than the particle size (circumference).

For the observer, upwelling (reflected or backscattered) and downwelling (transmitted) radiation outside the cloud we set $\tau = 0$ in Eq. (2) and $\tau = \tau_o$ in Eq. (1). The resulting solutions reduce to

$$I/I_o\Downarrow(\lambda) = [1-r_o^2]/[e^{k\tau_o} - r_o^2 e^{-k\tau_o}] - e^{-\tau_o}, \quad (6)$$

$$I/I_o\Uparrow(\lambda) = r_o[e^{k\tau_o} - e^{-k\tau_o}]/[e^{k\tau_o} - r_o^2 e^{-k\tau_o}]. \quad (7)$$

We will be using these two equations in analyzing the colors of the clouds. The second term in Eq. (6), $[e^{-\tau_o}]$, is the directly transmitted (unscattered) sunlight, which Adamson subtracts off. Thus his solutions are for the scattered light only. Also note that we have not included the boundary conditions of downwelling skylight or upwelling light from surface reflection.

If the limiting case of conservative scattering $\omega_o = 1$ is substituted directly into Eqs. (3) and (4) and then k and r are substituted into Eqs. (6) and (7), it might seem that the solutions are not correct. This is because when r goes to unity and k goes to zero, Eqs. (6) and (7) as they are written appear indeterminate, i.e., 0/0. However, the solutions are correct and yield well-behaved limits as we show in Appendix A.

4. Model Spectra and Colors

Figure 3 shows the downwelling radiation as a function of wavelength for a range of reference optical depths spanning thin through thick conditions: $\tau_o = 0.1$, 0.3, 1, 3, 10, and 30. Figure 4 shows the upwelling radiation for the same optical depths. There is a wide range of asymmetry parameters and single-scattering albedos in smoke particles with $0.4 < g < 0.8$ and $0.5 < \omega_o < 0.9$ [3]. As we shall see, however, the results are insensitive to reasonable changes in ω_o and g. In this model we have used $\omega_o = 0.6$ and $g = 0.6$, typical values [7]. By varying the values of g and ω_o, we found that qualitatively similar results were obtained for the observed ranges of ω_o and g. Figures 3 and 4 show the incident sunlight (thick dashed line), scaled in intensity to the image for comparison. The brightness scales are relative.

The spectral distributions for the downwelling/transmitted light in Fig. 3 are consistent with the observed color variations. When $\tau_o < 1$ (thin cloud) the scattered light is rather bluish. In this limit, the observed light is dominated by single scattering for which the scattering cross section rises steeply with decreasing wavelength [$\propto \lambda^{-4}$ as in Eq. (5)]. This strongly favors the blue end of the spectrum. As τ increases and the cloud becomes optically thick, the scattered light becomes dimmer and redder. Two factors come into play here. First, the shorter wavelength photons are more effectively reflected, leaving primarily the longer wavelength/redder photons to penetrate the cloud. Second, more scattering events are required for shorter wavelength photons to transmit through the cloud; this leads to a further deweighting of these photons due to the single-scattering albedo intensity factor, ω_0^n (n = number of scattering events to exit cloud). Only around $\tau = 1$–3 is the cloud colorless (white or gray). Figure 2 shows the upwelling/reflected radiation. As expected, it starts out quite blue and in the limit of high optical depth, it approaches the color of the incident sunlight, i.e., white. As the opacity is increased, the reflectivity of the longer wavelengths increases relative to the blue end of the spectrum. However, the reflectivity at any wavelength cannot exceed unity; thus, in the limit of unit reflectance at all wavelengths, the solar spectral distribution is observed.

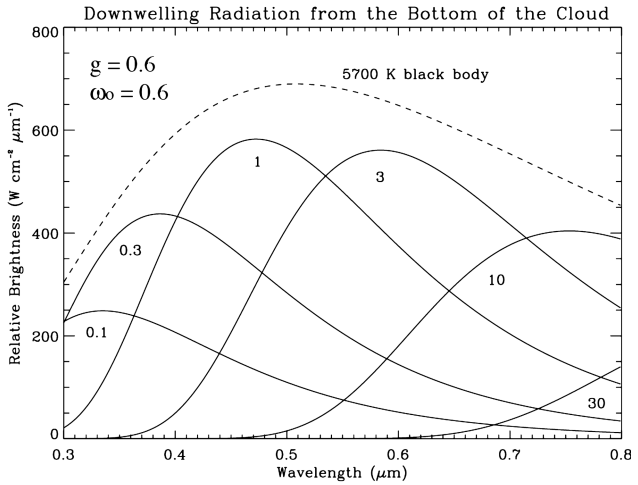

Fig. 3. Downwelling radiation: theoretical spectra of the clouds using a 5700 K blackbody as a source. Optical depths at 500 nm are 0.1, 0.3, 1.0, 3.0, 10, and 30. Note that for low optical depths the spectra peak in the blue part of the spectrum but with increasing optical depth, the peak wavelength shifts to the red end of the spectrum. As the optical depth exceeds about 3, the cloud appears redder and redder.

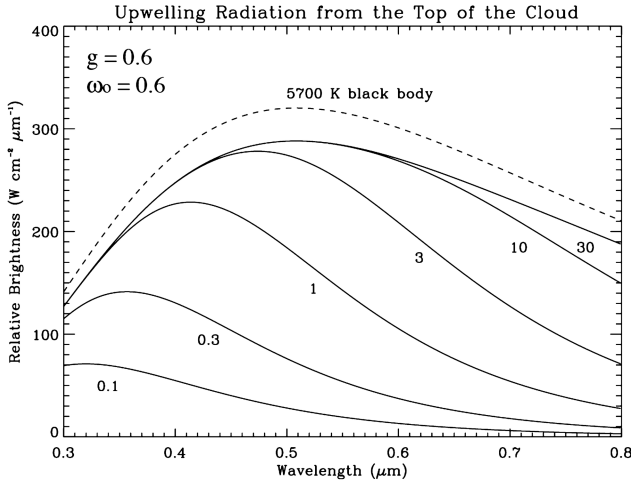

Fig. 4. Upwelling radiation: theoretical spectra of the clouds using a 5700 K blackbody as a source. Optical depths at 500 nm are 0.1, 0.3, 1.0, 3.0, 10, and 30. Note that for low optical depths the spectra peak in the blue part of the spectrum. With increasing optical depth, the peak wavelength shifts redward but saturates in the limit at the same color as the source: 500 nm. Such smoke appears white.

Figures 5 and 6 show the color coordinates for the model cloud spectra shown in Figs. 3 and 4, respectively. As the optical depth goes from small to large, the downwelling radiation starts out blue and ends up red. For a similar run of optical depths, the upwelling radiation starts out blue and ends up white, or more precisely, gray. In view of the qualitative observations and the ability to reproduce them within broad limits, it appears that the color variations of smoke clouds are fully represented by and understood within the context of a 1-D, two-stream radiative transfer model.

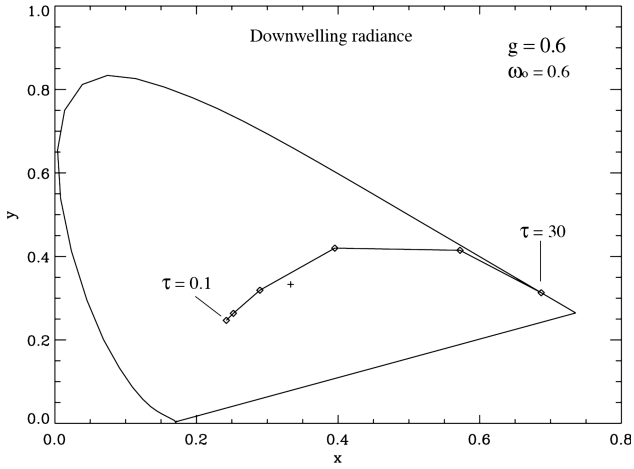

Fig. 5. CIE color diagram showing the color trajectories of downwelling (transmitted) radiation spectra from Fig. 3. The achromatic point is shown as a +. As the optical depths increase from 0.1 to 30, the apparent color of the cloud goes from bluish to reddish, in agreement with observations.

5. Discussion

Smoke particles from brush and forest fires have a surprisingly consistent range of properties. They are composed primarily of friable carbon with highly complex surfaces. They have been described by some as fractals. The main difference involves the amount of water that accumulates on or in the hygroscopic bits of soot.

The hotter the fire, the purer the carbon in the soot. Low temperatures leave carbonaceous compounds in the carbon, and in rare cases the soot is made almost entirely of polycyclic aromatic hydrocarbons. Very hot fires are often associated with high winds, where the airflow acts like a blast furnace to elevate the combustion temperature. In the case of the Day fire shown in Fig. 1, Southern California's Santa Ana winds were blowing. Such winds are hot and dry, with relative humidities as low as 2%. In such fires, accumulation of water is probably not significant.

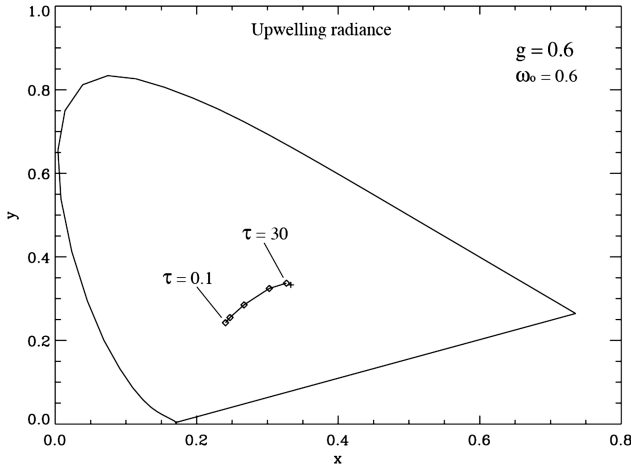

Fig. 6. CIE color diagram showing the color trajectories of upwelling radiation spectra from Fig. 4. The achromatic point is shown as a +. As the optical depths increase from 0.1 to 30, the apparent color of the cloud goes from bluish to white, in agreement with observations.

The results presented above are for a single pair of values for g and ω_o, which are representative of smoke particles. We have also explored the sensitivity of the results, particularly with respect to cloud color, of varying these parameters. If g is changed from 0.6 to 0 (the 1-D equivalent of the Rayleigh phase function), the color diagrams remain nearly identical. However, the intensity levels change, as expected, with an increase in the upwelling intensity and a decrease in the downwelling intensity. Increasing ω_o from 0.6 to 0.9 produces a slight reddening of the reference color and increases the intensity of both the upwelling and the downwelling fluxes. Decreasing ω_o from 0.6 to 0.3 produces a slight whitening of the reference color and decreases both fluxes. It is emphasized that, although these changes in ω_o are quite substantial, the reference color is essentially preserved and undergoes only a slight change in shading. We have also changed the wavelength dependence of ω_o from wavelength independent to a strongly wavelength-dependent form of $\omega_o \pm 1.0(\lambda - 0.6)$, which corresponds to a very strong red (+) or blue (–) albedo. This was found to only alter the shade of the color in the direction of the albedo color change. The key point is that the color of smoke clouds is relatively insensitive to g and ω_o and is primarily driven by the steep wavelength dependence (λ^{-4}) of the optical depth.

To reinforce the importance of Rayleigh-like scattering in determining the color of a cloud of any composition, we present a counterexample. Figure 7

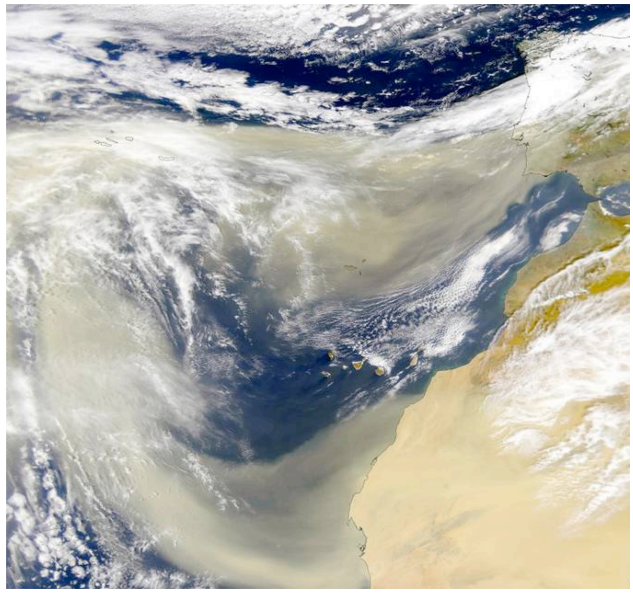

Fig. 7. (Color online) NASA SeaWiFS image of dust blowing west from the Sahara Desert over the Atlantic Ocean. Note that the dust color matches that of the sources, i.e., tan. This is because the dust particles are much larger than the wavelength of visible light and thus are not in the Rayleigh scattering regime. As a result, the dust's intrinsic color is evident and is due to the dust's chemical composition. Photograph courtesy of NASA.

shows a satellite view of windborne Sahara Desert dust blown over the Atlantic Ocean. The dust cloud is composed of particles that are much larger than the wavelength of light and thus are not strongly influenced by Rayleigh scattering. In this large particle limit, the color is driven by the wavelength dependence of ω_o, which reflects the color of the bulk material. As a result, the dust cloud appears the same color as the sand dunes from which they where blown. The color results from the chemical composition of the dust and thus appears distinctly brownish.

We noted earlier that the transmitted light in Fig. 1 displayed a large range of colors. This reflects the true 3-D nature of the situation, in contrast to our simplified 1-D representation. This particular smoke cloud is not highly optically opaque, which means that an observer looking directly at the Sun sees photons that either directly traverse the cloud or undergo just a few scattering events. This accounts for the slight blurring, high intensity, and "bluer" colors seen toward the Sun. As one looks at larger angles from the Sun, the downwelling photons have undergone more scattering events, corresponding to a larger effect optical depth (in our 1-D view). Thus, their intensity is much lower and their color is much redder than the more directly transmitted photons.

In our analysis above, we ignored the possible contribution of ambient light to the color of smoke clouds. The color and brightness of the terrain and the blue sky could influence the cloud color. We would not expect the terrain to be a major or even discernible factor because it would primarily affect the downwelling radiance. In view of the fact that typical albedos for terrain are relatively low $(0.05 - 0.4)$ and that the cloud is highly absorbing, terrain color and brightness reflected from the bottom of the cloud are not expected to play a significant role in the cloud's color.

The blue sky may have an influence for downwelling radiation, especially near the cloud edge where the optical depth is small. Here blue skylight will transit the cloud edge almost completely and thus should be indistinguishable from the blue light scattered by the cloud. The cloud will contribute its own blue component, but the relative contributions of either source are difficult to compute. It is possible that the edges of smoke clouds appear bluish because of their color contrast with the nearby adjacent reddish color from the optically thicker parts of the cloud.

For upwelling radiation, the blue sky's influence is not important for the following reason. Sunlight directly transmitted through the atmosphere is slightly reddened by Rayleigh scattering out of the beam. The blue that has been scattered out of the sunlight appears as a blue sky. When this blue sky illumination falls on the cloud, the blue component is "restored" to the slightly reddish direct sunlight and thus the total illumination of the cloud is "white."

Based on the fact that smoke particles are much smaller than the wavelength of light, we invoked a $1/\lambda^4$ dependence of the scattering cross section. Such an approach looks very much like a Rayleigh scattering situation. Pure Rayleigh scattering, however, would require that $g = 0$ and $\omega_o = 1$, and this is clearly not the case for smoke particles. Thus it is incorrect to claim that smoke particles behave as pure Rayleigh scatterers despite the fact that they are "Rayleigh-like" in some sense. From a parametric standpoint, it is likely that the exponent D of the wavelength dependence on scattering cross section falls in the range $-4 < D < -1$, where -4 corresponds to pure Rayleigh scattering and -1 corresponds to aerosols whose radii are near the wavelength of visible light. The agreement of our model using $D = -4$ and the observed properties of smoke clouds suggests that D is closer to -4 than to -1. Indeed, using $r = 0.1\,\mu$m and carbon's optical constants, our calculated Mie scattering cross section has a wavelength dependence of $D = -3.95$ in the visible part of the spectrum.

6. Summary and Conclusions

We have shown that the gross colors of light scattered from and through smoke clouds can be explained in terms of Rayleigh-like scattering and a 1-D multiple scattering radiative transfer model without regard to the actual composition of the smoke. The results are insensitive to the particles' single-scattering albedo and the asymmetry parameter, provided that these two quantities fall within broad ranges.

Appendix A

The downward flux [Eq. (6)] can be reexpressed as

$$F\downarrow + e^{-\tau_0} = \frac{(1+r_0)(1-r_0)}{e^{k\tau_0}(1+r_0e^{-k\tau_0})(1-r_0e^{-k\tau_0})},$$

which as 1-ω_0 becomes small is given by

$$F\downarrow + e^{-\tau_0} = \frac{(1-r_0)}{(1-r_0e^{-k\tau_0})}.$$

Noting that $e^{-k\tau_0} \to 1\text{-}k\tau_0$ and $r_0 \to 1$, this further simplifies to

$$F\downarrow + e^{-\tau_0} = \frac{1}{1+\frac{k\tau_0}{1-r_0}}.$$

After a little more algebra we find that

$$\frac{k\tau_0}{1-r_0} \to \frac{(1-g)\tau_0}{2}.$$

An analogous derivation will give the result for the upward flux [Eq. (7)]. In the end, we find the diffuse transmittance to be

$$T_{\mathrm{Dif}} = \frac{1}{1+\frac{(1-g)\tau_0}{2}} - e^{\tau_0}$$

and the diffuse reflectance to be

$$R = \frac{1}{1 + \frac{2}{(1-g)\tau_0}}.$$

As expected, the direct transmittance is

$$T_{\mathrm{Dir}} = e^{-\tau_0}$$

and $T_{\mathrm{Dif}} + T_{\mathrm{Dir}} + R = 1$, as it should be for the conservative scattering limit.

We are grateful to Craig Bohren for many useful discussions over the years regarding radiative transfer and multiple scattering. The authors are indebted to Alan Beeler for allowing us to use his photograph in Fig. 1. L. Bernstein appreciates the support of Spectral Sciences, Inc., by way of Independent Research and Development funding.

References

1. D. Adamson, "The role of multiple scattering in one-dimensional radiative transfer," NASA Tech. Note TN D-8084 (1975).
2. D. A. Chu, Y. J. Kaufman, C. Ichoku, L. A. Remer, D. Tanre, and B. N. Holben, "Remote sensing of smoke from MODIS airborne simulator during SCAR-B experiment," J. Geophys. Res. **103**, 31979–31987 (1998).
3. J. Wong and Z. Li, "Retrieval of optical depth for heavy smoke aerosol plumes: uncertainties and sensitivities to the optical properties," J. Atmos. Sci. **59**, 250–261 (2002) .
4. L. A. Remer, D. Tanré, Y. J. Kaufman, C. Ichoku, S. Mattoo, R. Levy, D. A. Chu, B. Holben, O. Dubovik, A. Smirnov, J. V. Martins, R.-R. Li, and Z. Ahmad, "Validation of MODIS aerosol retrieval over ocean," Geophys. Res. Lett. **29**, 8008, doi:10.1029/2001GL013204 (2002).
5. Y. J. Kaufman and T. Nakajima, "Effect of Amazon smoke on cloud microphysics and albedo-analysis from satellite imagery," J. Appl. Meteorol. **32** , 729–744 (1993).
6. O. Dubovik, B. N. Holben, Y. J. Kaufman, M. Yamasoe, A. Smirnov, D. Tanré, and I. Slutsker, "Single-scattering albedo of smoke retrieved from the sky radiance and solar transmittance measured from ground," J. Geophys. Res. **103**, 31903–31923 (1998).
7. E. I. Kassianov, T. P. Ackerman, J. C. Barnard, and C. J. Flynn, "Aerosol single-scattering albedo and asymmetry parameter from MFRSR observations during the ARM Aerosol IOP 2003," Atmos. Chem. Phys. Discuss. **6**, 13367–13386 (2006).